PRZEGLĄD ELEKTROTECHNICZNY

Ukazuje się od 1919 roku **10'2021**

Organ Stowarzyszenia Elektryków Polskich • **Wydawnictwo SIGMA-NOT Sp. z o.o.**

1. THABET Mohammed[1], 2. YSSAAD Benyssaad[1'], 3. LITIME EL Mostafa[2]

Ahmed Zabana University of Relizane Faculty of Science and Technology Department of Electrical Engineering and Automation
Laboratory: Industrial Engineering and Sustainable Development GIDD (1), Algeria
LAAS-National polytechnic school of Oran-Maurice Audin ENPO(2)
ORCID. 1. **0000-0001-7026-2119, 2. 0000-0002-4261-3070, 3. 0000-0002-4886-9800**

doi:10.15199/48.2021.10.01

A comparative study between PID and PD-SMC and PD-ASMC control applied on a delta robot

***Abstract**. This paper presents the modelling and control of a delta robot. The software SOLIDWORKS is used in this work to get a performing model that is very close to real system. The proportional integrator derivative (PID) control is used in this proposal. The results are compared with PD-Sliding mode (PD-SMC) and PD a robust SMC (PD-ASMC). This is an important comparative study where the advantages of each controller are presented: the PD-SMC improve the performance of the trajectory tracking, where the control signal performances and the robustness was improved by the PD-ASMC. Results presented are done with matlab-simulink and with Solidworks.*

***Streszczenie.** Atykuł przedstawia modelowanie i sterowanie robotem delta. Oprogramowanie SOLIDWORKS jest używane w tej pracy do uzyskania wydajnego modelu, który jest bardzo bliski rzeczywistemu systemowi. tak jak będziemy wyniki porównywane pomiędzy kontrolerami PID i (PD-SMC) i (PD-ASMC). Jest to ważne badanie porównawcze, w którym przedstawione są zalety każdego sterownika: PD-SMC poprawia wydajność śledzenia trajektorii, gdzie wydajność sygnału sterującego i odporność zostały ulepszone przez PD-ASMC. Przedstawione wyniki zostały wykonane za pomocą matlab-simulink oraz Solidworks. (**Badanie porównawcze sterowania PID i PD-SMC oraz PD-ASMC w robocie delta**)*

Keywords: Delta parallel robot, Dynamic model, trajectory tracking, PD-ASMC, RMSE.
Słowa kluczowe: Robot równoległy delta, model dynamiczny, śledzenie trajektorii, PD-ASMC, RMSE.

Introduction

Robots are now occupying lot of fields, including industrial, medical, etc. This importance prompted many researchers to work on solving the problem of tracking the trajectory and the increase in the accuracy of its work. In the old days, PID (proportional-integrator-derivative) was used due to its ease of application and acceptable performances [1]. But due to the complex dynamics of parallel robots and the requirement to optimize performances to follow complex trajectory, PID produces control signals not physically feasible. This has led many researchers to develop and improve PID results. The philosophy of nonlinear PD was to make the constants P and D variable by changing the error and this gives acceptable results but lacks robustness, due to its closed structure. This resulted in the insertion of robust controllers on PD including FUZZY LOGIC [2,3]and sliding mode control SMC. The PD-SMC controller gave better results in terms of control, performance, path following, and strength.

The goal of automatic control is to decrease control signals and increase performances. It is known that the mathematical model is somewhat far from the real system, which leads to a lack of robustness in the sliding mod control SMC. The SMC is known to have high vibrations in the control signals due to the “sign” function. The role of the constant I in the PID controller is to completely cancel the modeling error and the error signal, but in return it reduces the phase margin and this greatly affects the robots because they move along paths and need a large phase margin, which leads to destabilization of the system. This is what led to his absence. The absence of the constant I in the PID control and the presence of the sign function in the SMC makes the PD-SMC less robustness and the control signals are vibrational.

3dof Delta parallel robots are one of the most popular robots in the industry, which led to the application of many controllers, and due to their complex dynamics, it was the passion of many researchers, which prompted them to work on it a lot and apply linear and nonlinear controls, such as PD control [4], and linear control that was synthesised around an operating point [5,6], Adaptive control [7], PD-SMC and NPD-SMC [8], however, the above mentioned controllers are considered insufficient, and this was shown in the first paragraph in relation to PID, PD-SMC, NPD-SMC.

In this paper, we will create a model of the robot on SOLIDWORKS in order to represent the real system mechanically, and we will introduce a new controller, is called PD-ASMC, to solve the problem of tracking the trajectory, robustness and control signals. SMC is known to drag the model to the sliding surface, if they find a model error that affects a robustness of control, we will compensate for this by entering the error signals multiplied by the ratio of the modelling error in the sliding surface function (S), and after pulling the system to the sliding surface, the SMC takes it to the original with the “sign” function, and we will replace the “sign” with a “tanh” to reduce the vibrations of the control signals.

Finally, we conduct a comparative study between PID, PD-SMC and PD-ASMC in order to demonstrate the efficacy and high tracking performance of the PD-ASMC.

The structure of the article is as follows: In Section 2 a kinematics analysis of the robot will be studied, from which the inverse kinematics will be extracted and at the end of the section we will see the dynamic model of 3-DOF parallel robots. In Section 3, the PID and PD-SMC controller will be studied and designed, and we will address the errors of the controllers, and from them we will design the PD-ASMC controller. In Section 4 simulation tests are performed on the SOLIDWORK model to assess the accuracy and robustness of the controller. We will also study a comparison between the three controllers and the strength of the proposed controller will be demonstrated. We'll finish with the conclusion

Model of the DPR

Kinematics analysis

Delta parallel robots are known as complex systems due to their closed form, which affects the field of work where we find it small and limited and has a lot of singularities. In analytical kinematics we external the relation between the coordinates of x and ϑ [9,10]. We see in figures (1,2) [11] that the platform is connected with the arms l in the points P. We will take advantage of the length of the arms l and set it equal to the Euclidean norms as shown in the equation (1).

(1) $$J = \|l_i\| = l^2{}_{ix} + l^2{}_{iy} + l^2{}_{iz}$$

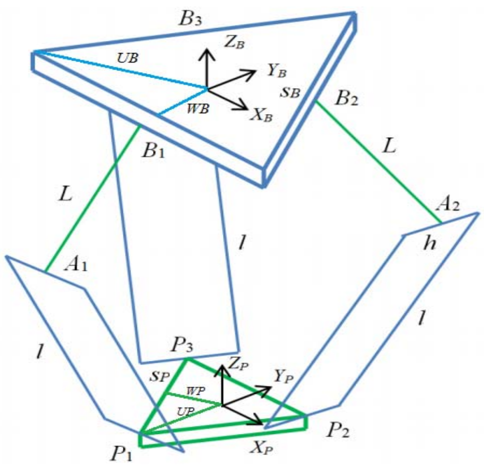

Fig.1. Delta parallel Robot

With knowing that $l_I{}^B$ is equal to the following

$$l_1{}^B = \begin{Bmatrix} x \\ y + L\cos\vartheta_1 \\ Z + L\sin\vartheta_1 \end{Bmatrix}$$

$$l_2{}^B = \begin{Bmatrix} x - \sqrt{\frac{3}{2}}L\cos\vartheta_2 + b \\ y - \frac{1}{2}L\cos\vartheta_2 + c \\ Z + L\sin\vartheta_2 \end{Bmatrix}$$

$$l_3{}^B = \begin{Bmatrix} x + \sqrt{\frac{3}{2}}L\cos\vartheta_3 - b \\ y - \frac{1}{2}L\cos\vartheta_3 + c \\ Z + L\sin\vartheta_3 \end{Bmatrix}$$

when analysing Equation 1, we extract the following

(2) $$E_i\cos\vartheta_i + F_i\sin\vartheta_i + G_i = 0$$

where

$$E_1 = 2L(y + a)$$

$$E_2 = -L(\sqrt{3}\,(x + b) + y + c)$$

$$E_3 = -L(\sqrt{3}\,(x + b) - y - c)$$

$$F_1 = F_2 = F_3 = 2zL$$

$$G_1 = x^2 + y^2 + z^2 + a^2 + L^2 + 2ya - l^2$$

$$G_2 = x^2 + y^2 + z^2 + b^2 + c^2 + L^2 + 2(xb + yc) - l^2$$

$$G_3 = x^2 + y^2 + z^2 + b^2 + c^2 + L^2 + 2(-xb + yc) - l^2$$

And

$$a = w_B - u_p,\quad b = \frac{1}{2}s_p + \frac{\sqrt{3}}{2}w_B,\quad c = w_p - \frac{1}{2}W_B.$$

The flowing figure 2 represent the Base and platform for the DELTA robot

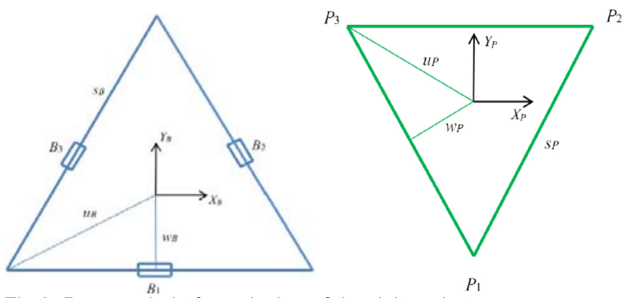

Fig.2. Base and platform design of the delta robot

Inverse kinematics

In this part, we will study the reverse movements of the robot. We will calculate ϑ by means of the x coordinates.in the equation (2) we can calculate the value of ϑ [12,13]. by changing a variable in this equation, as follows

$$q_i = \tan\vartheta_i \text{ then } \cos\vartheta_i = \frac{1 - q^2{}_i}{1 + q^2{}_i} \text{ and } \sin\vartheta_i = \frac{2q_i}{1 + q_i}$$

We will replace $\cos\vartheta$ and $\sin\vartheta$ with what they are equal to and substitute it into equation (2) and get the following equation

(3) $$(G_i - E_i)q_i{}^2 + (2F_i)q_i + (G_i + E_i) = 0$$

The solution of equation (3) is

(4) $$q_i = \frac{F_i \pm \sqrt{E_i^2 + F_i^2 - G_i^2}}{G_i - E_i}$$

And from it we extract ϑ

(5) $$\vartheta_i = 2\tan^{-1}(q_i)$$

We notice that the equation (5) has two solutions for each angle, one is positive and the other is negative, and from the combination of the three angles we extract 8 positions for the robot and all of it is corrects. But the dynamic of the robot forces us to choose one position, which is the positive angle.

Dynamic model of DPR

The dynamic model is the relationship between the torques (and / or forces) applied to the actuators and the articular positions, speeds and accelerations [14,15]. We represent the dynamic model by a relation of the form (6). Fig. 1 shows the schema of a 3-DOF delta parallel robot and in table 1 we find the architectural parameters of the robot extracted from SOLIDWORKS.

$$\tau = \mathrm{M}(\vartheta)\ddot{\vartheta} + \mathrm{C}(\vartheta,\dot{\vartheta})\dot{\vartheta} + \mathrm{G}(\vartheta) \quad (6)$$

where: τ – vector torque $\tau=[\tau_1,\tau_2,\tau_2]$, and ϑ – the joint vector $\vartheta=[\vartheta_1,\vartheta_2,\vartheta_3]$ and $\dot{\vartheta}$ $\ddot{\vartheta}$ – the speed and acceleration joint vector respectively.

$$M(\vartheta) = Ib + (mn + 3mab + 3mb)J^{'}J \quad (7)$$

M–the inertia matrix and $Ib = \mathrm{L}^2(\frac{1}{3}\mathrm{mb}+\mathrm{mc}+\frac{2}{3}\mathrm{mab})\mathrm{I}$ denotes the upper links inertial matrix.

$$\mathrm{C}(\vartheta,\dot{\vartheta}) = \mathrm{J}^{'}(\mathrm{mn}+3\mathrm{mab}+3\mathrm{mb})\mathrm{I}\frac{\mathrm{dJ}}{\mathrm{dt}}\dot{\vartheta} \quad (8)$$

C–vector resulting from Coriolis and centrifugal forces, I – represent the 3x3 identity matrix,

$$\mathrm{G}(\vartheta) = \mathrm{J}'(\mathrm{mn}+3\mathrm{mab})\mathrm{g} - \mathrm{L}(\mathrm{mb}/2+\mathrm{mc}+\mathrm{mab}/2)\,\mathrm{gcos}(\vartheta)) \quad (9)$$

is the gravity torque vector, and g the gravity acceleration, J is the Jacobin matrix that represents the relation between the articular and operational speed $\dot{\mathrm{x}} = \mathrm{J}\dot{\vartheta}$

Table 1. architectural parameters of the robot

name	meaning	value
mn	Moving platform	187.3(g)
mab	Lower arm	53.1(g)
mb	Upper arm	88(g)
L	Upper legs length	150(mm)
l	Lower legs parallelogram length	300(mm)
WB	planar distance from (0) to near base side	239.6(mm)
UB	planar distance from (0) to a base vertex	119,8(mm)
SB	Base equilateral triangle side	415(mm)
UP	planar distance from (P) to a platform vertex	49,65(mm)
WP	planar distance from (P) to near platform side	24,8(mm)
SP	platform equilateral triangle side	86mm

The inverse dynamic model represented by the relation of the form (6). The direct dynamic model is that which expresses the articular accelerations as a function of the positions, speeds and couples of the joints. It is then represented by the following relation:

$$\ddot{\vartheta} = \mathrm{M}(\vartheta)^{-1}(\tau - \mathrm{C}(\vartheta,\dot{\vartheta}) - \mathrm{G}(\vartheta)) \quad (10)$$

Controller design

PID control design

We will convert the robot system to a linear model as shown in Equation 11. And we will control its joints by the PID controller [16] as shown in Figure 3.

$$\tau = m_{\max}\ddot{\vartheta} + c_{\max}\dot{\vartheta} + g_{\max} \quad (11)$$

where $m_{\max}$, $c_{\max}$, $g_{\max}$ – the maximum value of the element M_{jj}, C_{jj} , G_{jj} Respectively

The controller law is shown as follows

$$\tau = K_p(\vartheta_d - \vartheta) + K_d(\vartheta_d - \vartheta) \quad (12)$$

The calculation of the three constants (K_p , K_I , and K_d) will be based on Khalil Domber method

$$K_{pjj} = 3m_{\max\,jj}W^2, K_{Ijj} = m_{\max\,jj}W^3,$$

$$K_{djj} = m_{\max\,jj}W$$

Where $m_{\max} = \begin{bmatrix} 0.05 & 0 & 0 \\ 0 & 0.05 & 0 \\ 0 & 0 & 0.05 \end{bmatrix}$

The frequency W is selected at $50rad/s$ Where

$$K_P = \begin{bmatrix} 375 & 0 & 0 \\ 0 & 375 & 0 \\ 0 & 0 & 375 \end{bmatrix} \quad K_I = \begin{bmatrix} 6250 & 0 & 0 \\ 0 & 6250 & 0 \\ 0 & 0 & 6250 \end{bmatrix}$$

$$K_d = \begin{bmatrix} 7.5 & 0 & 0 \\ 0 & 7.5 & 0 \\ 0 & 0 & 7.5 \end{bmatrix}$$

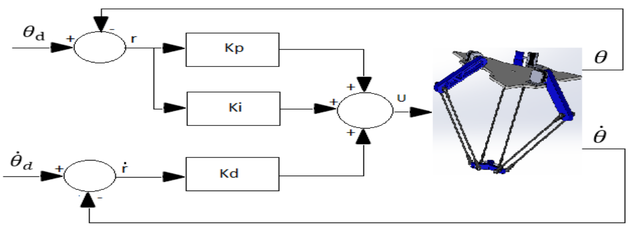

Fig. 3. Block diagram of the PID controller

PD-SMC control design

The PD control in this part will represent the sliding function, so as to ensure the trajectory tracking and the reduction in the modelling error [17], as shown in the following equation.

$$S = K_p e(t) + K_d \dot{e}(t) \quad (13)$$

The goal of the controller is to following the trajectory which means $\lim_{t\to\infty} e(t) = 0$. Based on this, and from the derivative of the sliding function we will extract the control unit as follows

$$\dot{S} = K_p \dot{e}(t) + K_d \ddot{e}(t) \quad (14)$$

where $\ddot{e}(t) = \ddot{\vartheta}_d - \ddot{\vartheta}$

Substituting equation (10) into equation (14), we obtain the continuous control unit shown as follows

$$\tau_c = (K_d M^{-1})^{-1}[K_p \dot{e}(t) + K_d \ddot{\vartheta}_d + K_d M^{-1}(c(\vartheta,\dot{\vartheta}) + G(\vartheta))] \quad (15)$$

In order to ensure the stability of the system along the path and in difficult situations, we will do this on through the LAYAPONOV function and we will extract the law of the discontinuous controller τ_d as shown.

(16) $$\dot{V} = S^T(t)\dot{S}(t) < 0$$

Guardian to ensure equation 2 is less than zero, $\dot{S}$ must be opposite to the S signal. Thus, we will add to the continuous control unit the discontinuous controller as shown as follows

(17) $$U = \tau_c + \tau_d$$

where $\tau_d = K sign(S)$,

PD-ASMC CONTROL DESIGN

In this part we will process τ_c and this is to compensate for the modeling error and to increase the robot performance, we will process τ_d and this is in order to improve the control signal[17], as shown below.

(18) $$S = K_p e(t) + K_d \dot{e}(t) + \xi(t)$$

where $\xi(t) = \beta e(t)^{\delta}$ β and δ are positive constants, we will increase the missing information by inserting the error in the sliding function which makes it more stable, looking for the constants representing the modeling error rate.

(19) $$\dot{S} = K_P \dot{e}(t) + K_d \ddot{e}(t) + \dot{\xi}$$

(20) $$\dot{S} = K_P \dot{e}(t) + K_d[\ddot{\vartheta}_d - M(\vartheta)^{-1}(\tau - C(\vartheta,\dot{\vartheta}) - G(\vartheta))] + \dot{\xi}$$

where $\dot{\xi}(t) = \delta\beta e(t)^{\delta-1}$

the continuous control unit shown as below

(21)
$$\dot{S} = (K_d M^{-1})^{-1}[K_P \dot{e}(t) + K_d \ddot{\vartheta}_d - K_d M^{-1}(C(\vartheta,\dot{\vartheta}) - G(\vartheta)) + \dot{\xi}]$$

In the discontinuous controller, we will replace the "sign" function with the "tanh" function to reduce the vibrations of the control signal the discontinuous control unit shown as follows

(22) $$\tau_d = K \tanh(S)$$

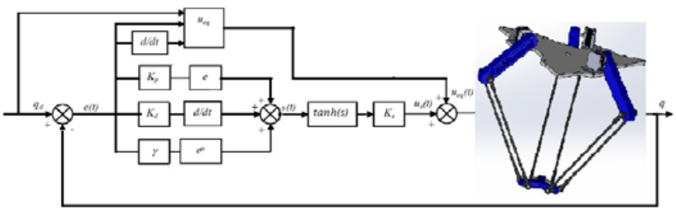

Fig.4. Block diagram of the PD-ASMC control

Simulation and results

In this part we will study and clarify the difference between controllers. We will choose a complex trajectory so that we can clearly see the difference between the three controls. To create the trajectory, we followed the quintic method and it would be flower shaped, as shown in Figure 5. We will design the controllers basing on mathematical models and apply them to the SOLIDWORKS as shown in Appendices. model in order to get an excellent study which is closer to reality.

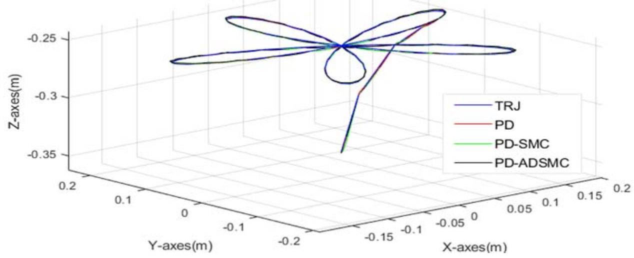

Fig.5. Operational trajectory tracking under the proposed Controller

The following diagrams illustrate the variation of the angular error in terms of time

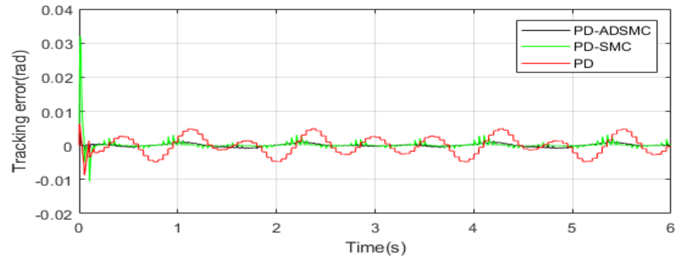

Fig.6. The tracking error for joint 1 (ϑ_1) under PID PD-SMC PD-ASMC control

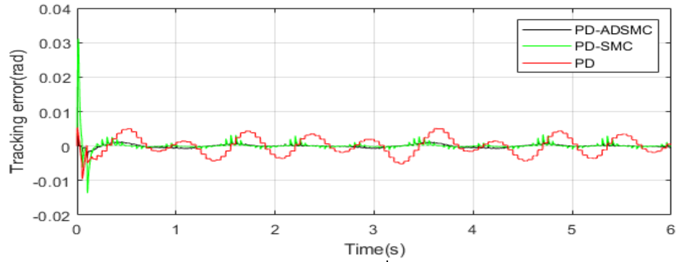

Fig.7. The tracking error for joint 2 (ϑ_2)under PID PD-SMC PD-ASMC control

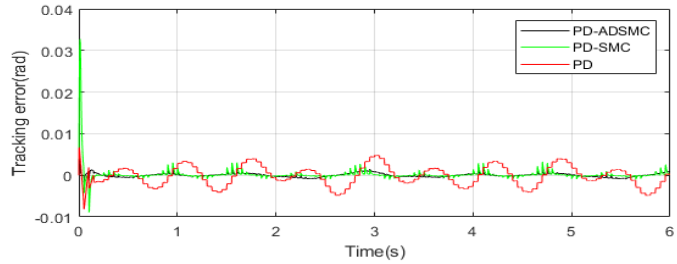

Fig.8. The tracking error for joint 3 (ϑ_3) under PID PD-SMC PD-ASMC control

From the three graph (6,7,8), we notice that the PID controller has acceptable results in tracking trajectory with a value of 0.005 rad as an upper bound, but for the PD-SMC controller initially we notice that it is moving away from the trajectory and that is due to the modeling error, but with the passage of time it gives better results than the PID. In the other hand, the PD-ASMC controller has excellent results throughout trajectory. From the above, we conclude that PD-ASMC gave better results in performance than PD-SMC, and the latter has better results than PID. To clarify more our study, we will deal with the use of the root means square error (RMSE) and take it as a performance indicator to prove the difference between them.

(23) $RMES_{\vartheta} = \sqrt{RMES_{\vartheta 1}{}^{2} + RMES_{\vartheta 2}{}^{2} RMES_{\vartheta 3}{}^{2}}$

With

$$RMES_{\vartheta 1} = \sqrt{\frac{1}{n}\sum_{i=1}^{n} e_{\vartheta 1}}$$

where $RMES_{\vartheta}$ $e_{\vartheta 1} = (\vartheta_{d1} - \vartheta_{1})$

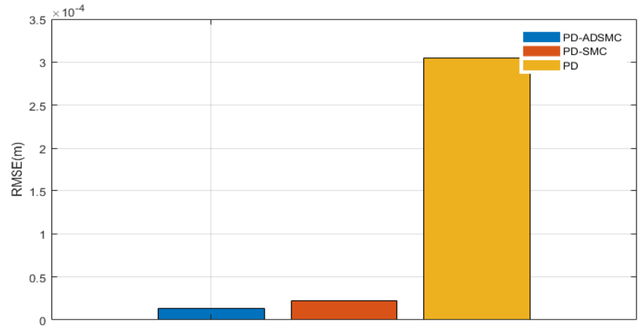

Fig.9. The RMSE diagram under PID PD-SMC PD-ASMC control

Note from the previous figure the PD-ASMC improved RMSE by approximately 95% compared to PID and 30% compared for PD-SMC.

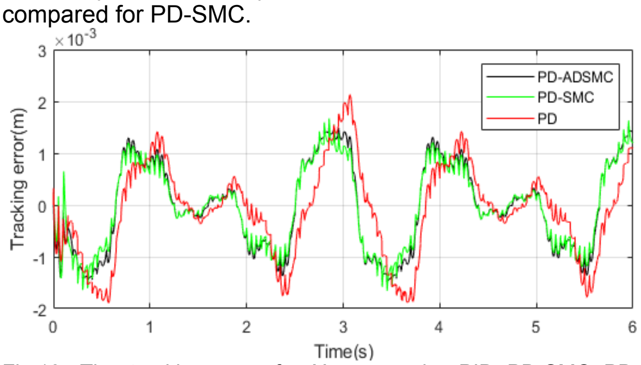

Fig.10. The tracking error for X-axes under PID PD-SMC PD-ASMC control

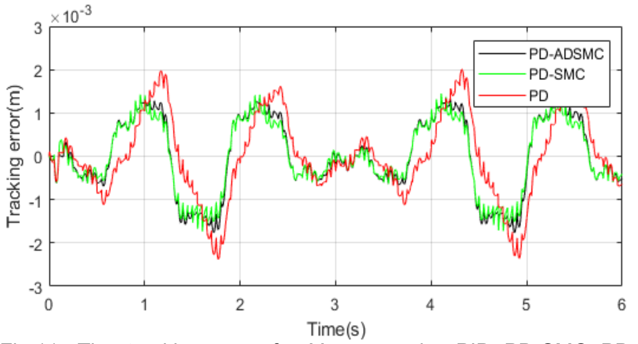

Fig.11. The tracking error for Y-axes under PID PD-SMC PD-ASMC control

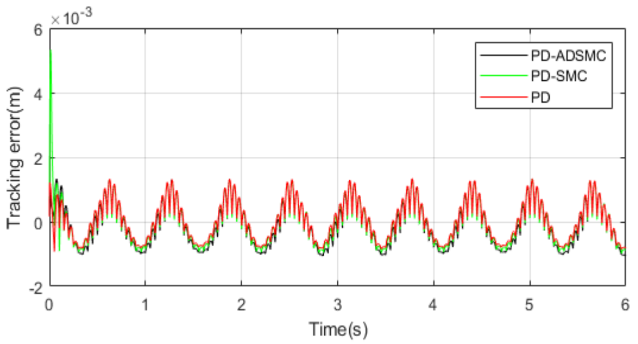

Fig.12. The tracking error for Z-axes under PID PD-SMC PD-ASMC control

As for the operating area representing in the figure (10,11,12), we notice that the three controls have similar results along the trajectory, but the performance of PD-ASMC remains better than that of PD-SMC and this is clearly shown in Z-axes and is better than PID in the three coordinates

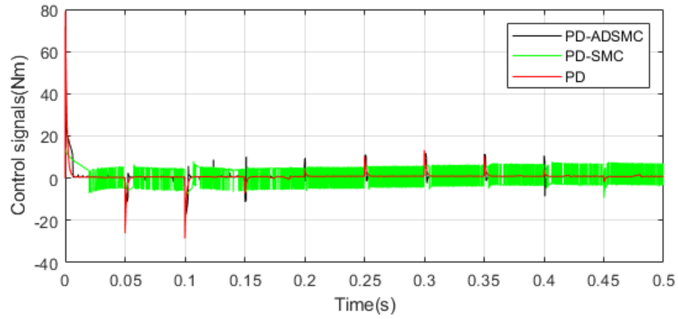

Fig.13. The control signals for joint 1 (ϑ_1)under PID PD-SMC PD-ASMC control

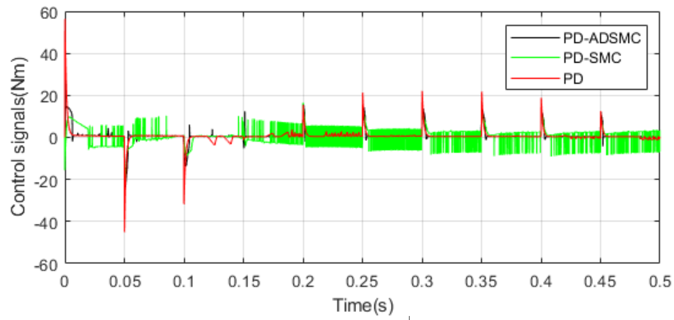

Fig.14. The control signals for joint 2 (ϑ_2)under PID PD-SMC PD-ASMC control

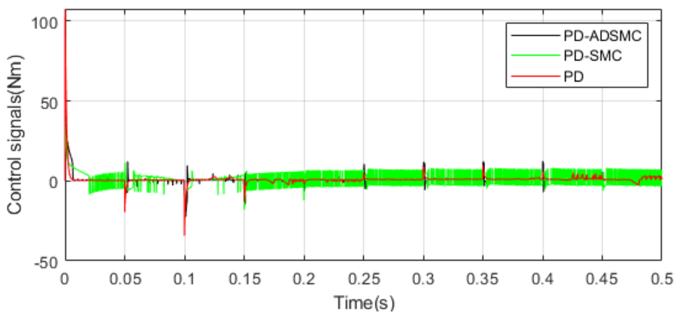

Fig.15. The control signals for joint 3 (ϑ_3) under PID PD-SMC PD-ASMC control

Table 2. The parameters of PID PD-SMC PD-ASMC

	K_p	K_d	K_I	β	δ
PID	375	7.5	6250	\	\
PD-SMC	375	7.5	/	\	\
PD-ASMC	375	7.5	/	4	2

From the graphs (13,14,15), is clear that the PID controller produces a control signal that exceeds 100 Nm in terms of amplitude, to achieve the performance that we have seen in graphs 4,5and 6, and this signal can be physically produced and from it we conclude that this performance achieved by the PID can be seen in reality. On the other hand, PD-SMC produced an excellent control signal in terms of amplitude. We see that it ranges between -15Nm and 15Nm, but has very large vibration, which is a result of the "sign" function. Similarly, due to the complexity of the trajectory, PD-ASMC produces an excellent control signal in terms of amplitude and vibration, where the amplitude of the control signal exceeds 20 and the vibrations are almost non-existent.

CONCLUSION

We have seen in this paper a new path in simulation where we have created a real model of a DELTA parallel robot on SOLEDWORKS, and this may help us to know the power of the controller and the performance resulting from it. It is known that the nonlinear mathematical model of a system is far from the real system, this leads researchers to adjust the parameters in the control unit to make it work on the truth system. We also saw a new control method in the field of DELTA ROBOT, which is PD-ASMC, where the results were good in terms of performance and control signal. PD gave good results in terms of performance, but it cost a lot of control signal in term of amplitude, where PD-SMC was better than it, but it contains big vibrations in the control signal, to correct this disadvantage we created the PD-ASMC controller.

Appendix

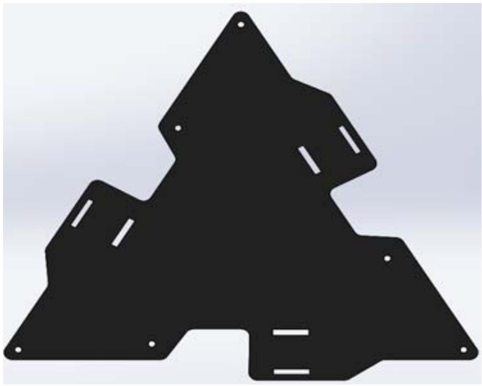

Fig.16. fixed base

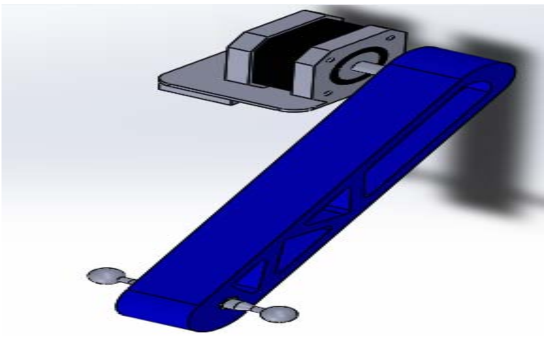

Fig.17. upper arm

Fig.18. lower arm

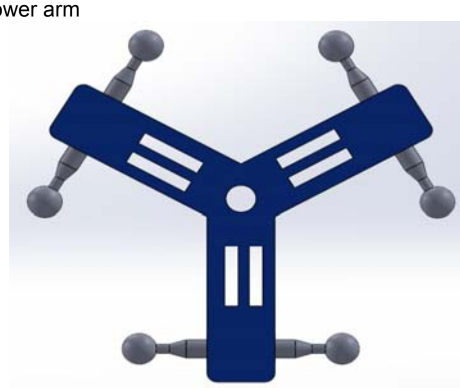

Fig.19. moving platform

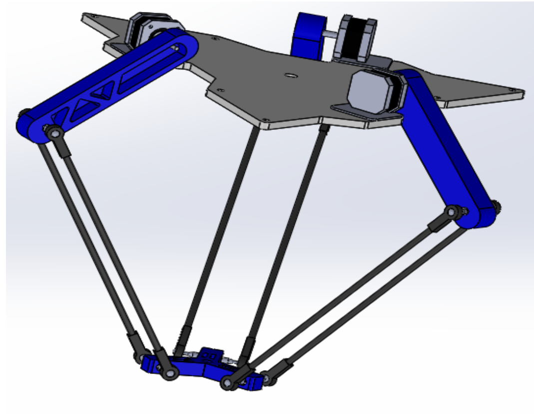

Fig.20. Delta Robots design

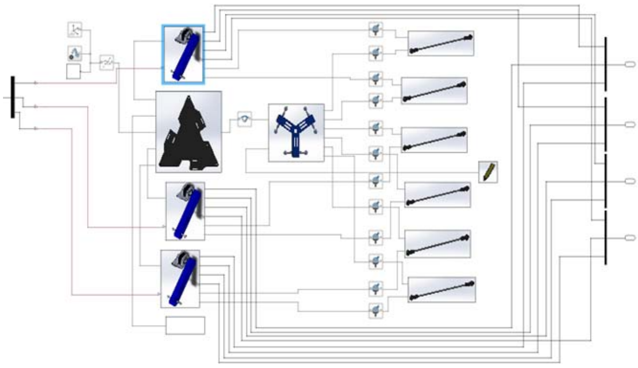

Fig.21. Model of delta robot in Simulink MATLAB

ACKNOWLEDGEMENT

Our special thanks to the examiners for their constructive comments. The authors are grateful to the General Direction of Scientific Research and Technological Development GDRSDT, Ministry of Higher Education and Scientific Research of Algeria for its continuous assistance in scientific research.

***Authors**: PhD student THABET Mohammed AHMED ZABANA University of relizane, department of automatic, E-mail: mohamedthabet093@gmail.com; Dr YSSAAD Benyssaad AHMED ZABANA University of relizane, E-mail: benyssaad.yssaad@cu-relizane.dz. Dr LITIME Mostafa ENPO-Oran E-mail lit_ldee@yahoo.fr.*

REFERENCES

[1] F. H. Ghorbel, O. Chetelat, R. Gunawardana, and R. Longchamp, “Modeling and set point control of closed-chain mechanisms: Theory and experiment,” IEEE Trans. Control Syst. Technol., vol. 8, no. 9, pp. 801–815, Sep. 2000

[2] O. Linda and M. Manic, “Uncertainty-robust design of interval type-2 fuzzy logic controller for delta parallel robot,” IEEE Transactions on Industrial Informatics, vol. 7, no. 4, pp. 661–670, 2011.

[3] Lu, X.G.; Liu, M.; Liu, J.X. Design and Optimization of Interval Type-2 Fuzzy Logic Controller for Delta Parallel Robot Trajectory Control. Int. J. Fuzzy Syst. 2017, 19, 190–206.

[4] A. Codourey, ”Dynamic modelling and mass matrix evaluation of the delta parallel robot for axes decoupling control”, International Conference on Intelligent Robots and Systems, vol.3, pp.1211-1218, 1996.

[5] M. Rachedi, B. Hemici and M. Bouri, ”Design of an H1 controller for the Delta robot: experimental results”, Advanced Robotics, vol.29, no.18, pp 1165-1181, 2015.

[6] J. Fabian, C. Monterrey, and R. Canahuire, "Trajectory tracking control of a 3 DOF delta robot: a PD and LQR comparison," in IEEE International Congress onElectronics, Electrical Engineering and Computing (INTERCON), 2016, pp. 1-5.

[7] J. Cazalilla, M. Valles, V. Mata, M. Diaz-Rodriguez, A. Valera, Adaptive control of a 3-DOF parallel manipulator considering payload handling and relevant parameter model, Robot. Comput.-Integr. Manuf. 30 (5) (2014) 468–477.
[8] C. E. Boudjedir, D. Boukhetala, and M. Bouri, "Nonlinear PD plus sliding mode control with application to a parallel delta robot," Journal of Electrical Engineering, vol. 69, pp. 329-336, 2018.
[9] Mohsen Asgari, Mahdi Alinaghizadeh Ardestani, and Mersad Asgari, "Dynamics and control of a novel 3-DoF spatial parallel robot." In Proceedings of the 1st RSI/ISM International Conference on Robotics and Mechatronics, pp. 183-188, 2013.
[10] PK lamwal, SQ Xie, YH Tsoi, KC Aw, "Forward kinematics modelling of a parallel ankle rehabilitation robot using moditied fuzzy inference, " Mechanism and Machine Theory, vol. 45, pp.1537 - 1554, 2010.
[11] W. Khalil, O. Ibrahim, "General solution for the dynamic modeling of parallel robots, "Journal of Intelligent and Robotic Systems, vol. 49, pp. 19-37, 2007.
[12] M.A. Laribi, L. Romdhane, S. Zeghloul, Analysis and dimensional synthesis of the DELTA robot for a prescribed workspace, Mech. Mach. Theory 42 (7) (2007) 859–870
[13] H Hadfield, L Wei, J Lasenby "The Forward and Inverse Kinematics of a Delta Robot." University of Cambridge, Springer.2020
[14] M. Ö. Efe, "Fractional fuzzy adaptive sliding mode control of a 2 DOF direct drive robot arm," IEEE Trans. Syst., Man, Cybern., Part B: Cybern., vol. 28, no. 6, pp. 1561–1570, Dec. 2
[15] . M. Diaz-Rodriguez, A. Valera, V. Mata, and M. Valles "Model-Based Control of a 3-DOF Parallel Robot Based on Identified Relevant Parameters," Mechatronics, IEEE/ASME Transactions on, vol. 18, pp 1737-1744,2013
[16] Khalil W, Dombre E. Modeling identification and control of robots. London: Hermes, Penton Science; 2002
[17] Rahmani M, Komijani H, and Rahman M. New sliding mode control of 2-DOF robot manipulator based on extended grey wolf optimizer. Int J Control Auto Syst 2020; 18(X): 1–9.